

Development and Validation of a Wind Turbine Generator Simulation Model

Gordon E. North Piegan III, Rachid Darbali-Zamora and Jon C. Berg

Sandia National Laboratories, Albuquerque, New Mexico, 87185, USA

Abstract – This paper presents a type-IV wind turbine generator model developed in *MATLAB/Simulink*. An aerodynamic model is used to improve an electromagnetic transient model. This model is further developed by incorporating a single-mass model of the turbine and including generator torque control from an aerodynamic model. The model is validated using field data collected from the Scaled Wind Farm Technology (SWiFT) facility. The model takes wind speed as an input. The nacelle wind speed is known to have additional measurement and process noise. To ensure the model and SWiFT are compared accurately the nacelle wind speed is estimated using a Kalman filter. Simulation results show that using a single-mass model instead of a two-mass model for aerodynamic torque, including generator torque control from SWiFT estimating the wind speed via the Kalman filter and tuning the synchronous generator to match SWiFT. The model can accurately represent the generator torque, speed, and power.

Keywords – wind turbine generator, aerodynamic, electromagnetic transient

NOMENCLATURE

A_{rotor}	Rotor area
β	Pitch angle
$C_p(\lambda, \beta)$	Power coefficient
H	Inertia time constant
J	Inertia
J_r	Rotor inertia
MVA_{rated}	Rated power
P_{mec}	Mechanical power
P_e	Electrical Power
$GRatio$	Gear box ratio
T_a	Aerodynamic torque
λ	Tip-speed ratio
U	Wind speed
T_g	Generator torque
T_L	Torque losses
T_e	Electrical torque
ω_n	Rated generator speed
ω_r	Rotor speed
ω_g	Generator speed
$\hat{\omega}_g$	Generator at full speed
K_d	Damping coefficient synchronous generator
ρ	Air Density

I. INTRODUCTION

To help reduce harmful carbon dioxide (CO_2) emissions, more renewable energy sources (RES) such as wind turbine generators (WTGs) are being integrated into the electric grid to replace conventional generation sources, decreasing the dependency on fossil fuel. With an increasing role of wind power, there is a need for developing reliable simplified WTG models that can capture the aerodynamics as well provide analysis of electromagnetic transients (EMT). These WTG models can be used to help identify any adverse effects that may occur when interconnecting these large generation sources into the power grid [1]. While modeling WTGs remains a challenge, field data can aid in developing and validating models that can adequately capture a WTGs dynamic performance [2].

Herein, a *MATLAB/Simulink* power system simulation model that represents the EMT and aerodynamics of a WTG is presented. Both EMT and aerodynamic models have been shown to have drawbacks. The proposed solution is to model power more accurately by combining the aerodynamic model with the EMT model. The aerodynamic model will provide more accurate generator torque. And the EMT model will provide more accurate generator speed. The hybrid model will replace the EMT models 2-mass model with a single-mass model to improve aerodynamic torque and include generator torque control to obtain accurate generator torque. It will also replace the synchronous generator. Field measurements used for comparison were collected from the Scaled Wind Farm Technology (SWiFT) facility, located in Lubbock, Texas, are used to validate the simulation model. True wind speed in front of the rotor is unavailable, Nacelle measured wind speed from SWiFT is used as an input to the models. Nacelle wind speed is known to have noise due to disturbances and wake effect. A Kalman filter estimates the true wind speed to ensure that the generator speed, generator torque and generator power seen at the SWiFT WTG can be accurately represented by the model. Previous papers used known wind speeds with known noise characteristics. This paper will seek to estimate the true wind speed without such knowledge

II. WIND TURBINE GENERATOR DYNAMICS

WTGs convert the wind's kinetic energy into mechanical energy and then generators are used to convert this to electrical power. The relationship between a WTGs output power and wind speed is represented by their power curve. Fig. 1 illustrates an example of a typical WTG power curve. Depending on the wind speed, a WTG can operate under four regions within the power curve.

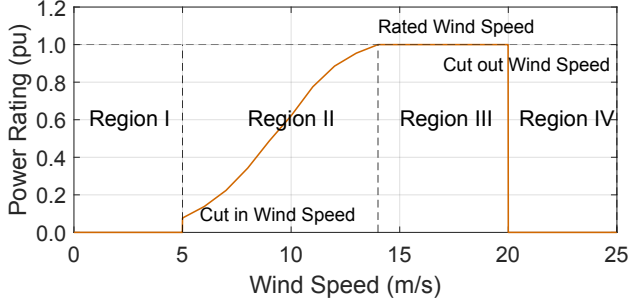


Fig. 1. Wind turbine generator power curve.

At region I, the generator torque is zero, $T_g = 0$, operating below cut in wind speed. At region II the cut in wind speed is reached and aerodynamic torque is approximated by equation (1).

$$T_a = \frac{\rho \cdot \pi \cdot R^3 \cdot U^2 \cdot C_p}{\lambda} \#(1)$$

In this equation variables ρ , R , U , λ , and C_p are air density, rotor radius, wind speed, tip speed ratio, and power coefficient, respectively. During region II the rotor speed changes as a function of the difference between aerodynamic torque, $GBratio$ of generator torque and torque losses divided by rotor inertia equation (2).

$$J_r \cdot \frac{d\omega_r}{dt} = T_a - \frac{GBratio}{T_g} - T_L \#(2)$$

In this equation, the variable $GBratio$ is the gear box ratio, T_L is torque losses, J_r is rotor inertia and $d\omega_r/dt$ is the change in rotor speed per unit time. When the generator torque, T_g and generator speed, ω_g increase, the power output reaches the rated power. The mathematical representation for the electrical power is shown in equation (3).

$$P_e = T_g \cdot \omega_g \#(3)$$

At rated power, operating in region III, the WTG adjusts the pitch to maintain a steady output of power. This occurs until the maximum rated wind speed is reached at region IV where the WTG stops producing power.

III. WIND TURBINE GENERATOR MODELING

Typical WTG modeling approaches rely on aerodynamic models [8], or EMT models [3]. Aerodynamic models have shown to be reliable in modeling WTGs and wind farm characteristics such as generator torque, generator speed and generator power [8], however these models do not include grid interconnections making them insufficient in representing load or fault conditions. EMT models can accurately depict grid interconnection interactions, allowing EMT models to accurately depict load or fault conditions at the generator [3]. In most EMT models there is a model of the turbine and drive train, however it does not include logic control of generator torque. Therefore, a model that accurately represents generator torque dynamics is needed. The aerodynamic model has a

control strategy which is the same as the control for the SWiFT facility WTGs. The single-mass model which yields aerodynamic torque allows for simplification because the parameters necessary for a two-mass model are unavailable.

In [5] a widely accepted method for model validation of a WTG is presented. To accomplish this validation, model adequacy is determined by using SWiFT WTG field measurements of generator torque, generator speed and generator power as target values to determine the effectiveness of obtaining aerodynamic torque via the single-mass model, generator torque via the SWiFT logic generator torque control, and tuning the damping coefficient of the SG to match generator speed and power.

A. Electromagnetic Transient Model

For this simulation, the EMT model used is a type-IV WTG. A type-IV WTG is defined as a full converter wind turbine (FCWT) which employs a SG, a three-phase rectifier, a DC-DC boost converter (average model), a three-phase inverter (average model), an RLC filter and a three-phase transformer [6]. Fig. 2 illustrates the block diagram for the WTG model. The kinetic energy from the wind is converted to mechanical energy via the turbine. This mechanical energy is converted to electrical energy using the SG, which then goes through the three-phase rectifier circuit, a DC/DC boost converter and then through a three-phase inverter. Finally, it is filtered using an RLC filter. The mechanical energy produced by the turbines is shown in equation (4).

$$P_{mec} = \frac{\rho}{2} \cdot A_{rotor} \cdot U^3 \cdot C_p(\lambda, \beta) \#(4)$$

In this equation, the variable P_{mec} is the mechanical power extracted from the wind, ρ is the air density in kg/m^3 , A_{rotor} is the area of the rotor in m^2 , U is the wind speed measured in m/s [4] and $C_p(\lambda, \beta)$ is the power coefficient a function, where variables λ and β are the tip speed ratio and the pitch angle in degrees, respectively. $C_p(\lambda, \beta)$ is commonly derived using an approximation equation found in [6]. The turbine transfers the mechanical power to the drive train which converts the mechanical power into mechanical torque [3]. The mechanical power is then converted to electrical power as shown in [3]. However, the proposed model replaces the induction machine with a SG.

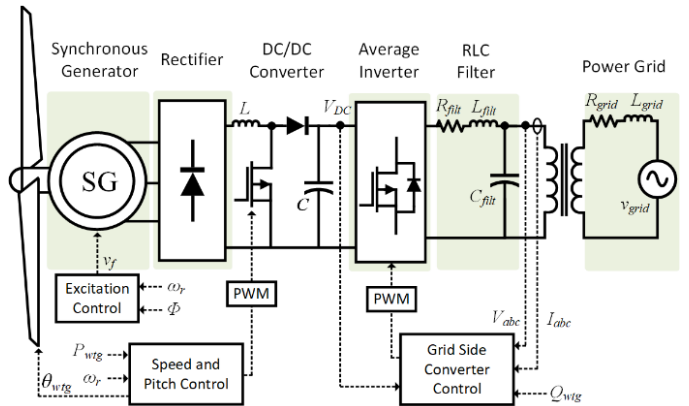


Fig. 2. Block diagram of the type-IV wind turbine generator.

B. Aerodynamic Model

Fig. 3 depicts the block diagram for the aerodynamic model which accurately represents the control logic and power coefficient of the SWiFT WTG. This model relies on the difference in generator torque and aerodynamic torque to yield generator and rotor speed. The aerodynamic model uses a look-up table for the SWiFT WTG $C_p(\lambda, \beta)$.

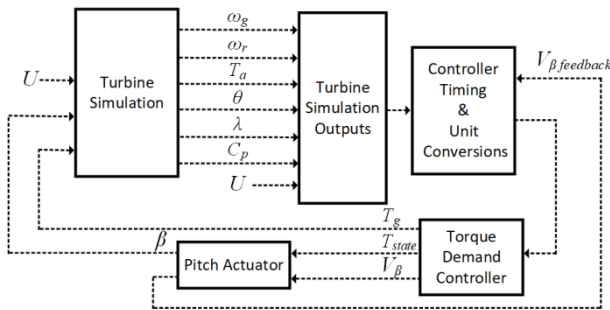


Fig. 3. Block diagram for the aerodynamic model.

C. Electromagnetic Transient and Aerodynamics Model

The aerodynamic model developed at Sandia is known to accurately predict generator power, speed, and torque. The EMT model is thus adjusted to match the aerodynamic model. Without sacrificing grid interconnection capabilities, the EMT model replaces the 2-mass model from [3] and uses the aerodynamic model's single mass model as values weren't available to use the 2-mass model. This provides a more accurate representation of T_a because $C_p(\lambda, \beta)$ is calculated with real data captured from SWiFT in a lookup table while [6] fits data to a curve. Fig 4a. Shows the power coefficient equation derived in [6] and figure 4b shows the power coefficient from the lookup table. A clear discrepancy exists around $\beta = 0$. The EMT model had no generator torque control, the generator torque control from the aerodynamic model is applied to yield accurate generator torque.

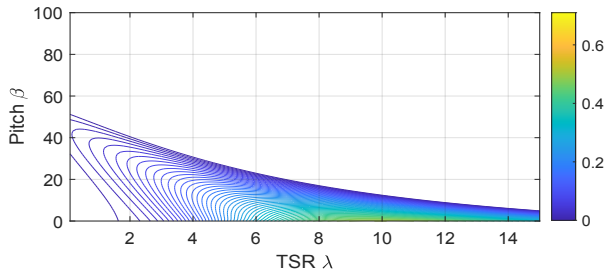


Fig. 4a. $C_p(\lambda, \beta)$ curve from equations summarized in [6].

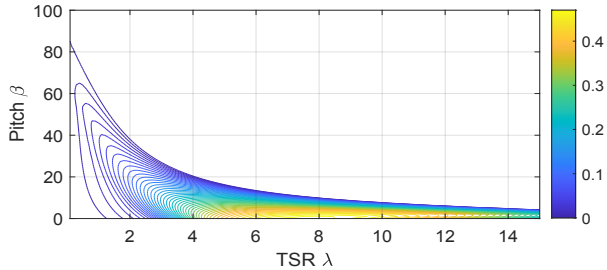


Fig. 4b. $C_p(\lambda, \beta)$ curve obtained from the look-up table.

Next, the EMT model replaces the original SG with a simple SG. Since the input torque to the SG is inherited from the aerodynamics model, the only difference in the EMT model affecting generator power is generator speed via equation (2). Generator speed defined by the simplified SG is summarized in equation (6) and equation (7).

$$\Delta\omega_g(t) = \frac{1}{2 \cdot H} \cdot \int_0^t (T_g - T_e) - K_d \cdot \Delta\omega_g(t) dt \#(6)$$

$$\omega_g(t) = \Delta\omega_g(t) + \hat{\omega}_g(t) \#(7)$$

Where, $\hat{\omega}_g$, is the generator speed at full load. The closed loop control diagram for the generator speed developed within the simplified SG is shown in Fig. 5.

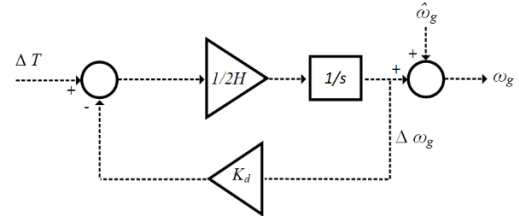


Fig. 5. Block Diagram for Traditional Control.

It can be deduced that H acts as an integral gain referred to as K_H . The block diagram of the control system depicts the difference in generator torque and mechanical torque. The transfer function that represents the control in Fig. 5 is summarized in equation (8).

$$\frac{\Delta\omega_g(t)}{\Delta T} = \frac{K_H}{s + K_d \cdot K_H} \#(8)$$

The integral gain K_H is a fixed constant and the damping ratio can increase the speed of the single pole. In turn the system has the ability to react to changes. The tuning process to determine the accurate damping coefficient required setting the internal resistances $R = 0.02$, $X_d = 0.3$, and the damping coefficient $K_d = 0$, and slowly ramping the damping coefficient until the generator speed accurately represent the SWiFT WTG.

Consider the Park's equations which define a SG from [13], as shown in equations (9) through equations (11).

$$T_e = \psi_q \cdot i_d - \psi_d \cdot i_q \#(9)$$

$$\psi_q = -(L_{m1} + L_l) \cdot i_d + L_{mq} \cdot i_{kq} + L_{mq} \cdot i_{fq} \#(10)$$

$$\psi_d = -(L_{md} + L_l) \cdot i_d + L_{md} \cdot i_{kd} + L_{md} \cdot i_{fd} \#(11)$$

The simplified model ignores the self and magnetizing inductances of the armature, field, and damper windings. The internal voltage V_f to ψ_d direct axes synchronous machine circuit, will thus be only the resistance and reactance in series. Meaning that a change in the resistance or reactance will result in an equivalent reduction or rise in electric torque. The effect is equivalent to tuning K_d . Let $C = R + X_d = K_d$, this yields equation (12) and equation (13).

$$\Delta\omega_g(t) = \frac{1}{2 \cdot H} \int_0^t (T_g - C * T_e) - C \cdot \Delta\omega_g(t) dt \#(12)$$

$$\Delta\omega_g(t) = \frac{1}{2 \cdot H} \cdot \int_0^t T_g dt \#(13)$$

A reduction in resistance or reactance will result in an increase in generator speed and vice versa for the simplified SG model.

IV. KALMAN FILTER WIND ESTIMATION

Accurate wind speed information is required to represent the true tip speed ratio, power coefficient and pitch. This value directly impacts the aerodynamic torque as well as the output power of the WTG. Wind speed measurements captured at the nacelle can add inaccuracies due to wake effects and machine noise [14, 15]. Moreover, a single measurement point is not realistic as the wind speed is captured across the entire rotor [14, 15]. A Kalman filter can be used to accurately estimate wind speed [15]. As the Kalman filter is typically used to measure an unknown state or to obtain a more accurate measurement of a known state. The wind speed will be solved by obtaining the unknown state of the aerodynamic torque, then using the Newton-Raphson method, the tip speed ratio is obtained [15]. Finally, the relationship between tip speed ratio, rotor radius and the filtered rotor speed is used to solve for wind speed. The drive train equation is shown in equation (2). The state space equations that describe the torque and speed is shown in equation (15) and equation (16) [16].

$$\begin{bmatrix} \dot{\omega}_r \\ \dot{T}_a \end{bmatrix} = \begin{bmatrix} 0 & 1 \\ 0 & J_r \\ 0 & 0 \end{bmatrix} \cdot \begin{bmatrix} \omega_r \\ T_a \end{bmatrix} + \begin{bmatrix} -\frac{GBRatio}{J_r} \\ 0 \\ 0 \end{bmatrix} \cdot T_g + w \#(15)$$

$$y = [1 \ 0] \cdot \begin{bmatrix} \omega_r \\ T_a \end{bmatrix} + v \#(16)$$

In these equations, variables v and w are the measurement noise and process noise characteristics, respectively. The process noise and measurement noise covariance matrices are chosen in order to satisfy equation (17) and equation (18).

$$E\{w(t) \cdot w^T(t)\} = Q(t) \#(17)$$

$$E\{v(t) \cdot v^T(t)\} = R(t) \#(18)$$

The initial measurement noise covariance and the process noise covariance matrix are shown in equation (19) and equation (20).

$$R = 10 \cdot 10^{-2} \#(19)$$

$$Q = \begin{bmatrix} 10 \cdot 10^{-2} & 0 \\ 0 & 6 \cdot 10^6 \end{bmatrix} \#(20)$$

While [15] used a known wind speed input and had the ability to choose the noise covariance, this analysis only utilizes the nacelle measurement. A true measurement of the process noise

and measurement noise covariances is typically unavailable, but methods exist to find a reasonable estimate [17]. The state-space equation from (15) is unstable. It is possible to track the states of a non-stable system [18] and using the relationship derived in equation (2) it is possible to determine a range of the aerodynamic torque. The Kalman filter yields the results for the aerodynamic torque and rotor radius. A non-linear equation can be derived where the tip speed ratio is the only unknown variable [16], as shown by equation (21).

$$\frac{C_p}{\lambda^3} = \frac{2 \cdot T_a}{\rho \cdot \pi \cdot R^3 \cdot U^2 \cdot \omega_r^2} \#(21)$$

The tip speed ratio is solved using Newton-Raphson rather than a look-up table. A look-up table is most reliable when calculating the aerodynamics of the system given the inputs are not approximations, but measured values. Because the values of the right-hand side of (22) are approximate estimates and because the lookup table has values which are close, the tip speed ratio was shown to oscillate and at times yield values out of range. Therefore, linear interpolation is used instead to find tip speed ratio, in [19] a variety of power coefficient models are provided. The sinusoid provides an accurate solution but may also cause oscillatory behavior outside the range of possible tip speed ratio. To prevent this behavior the tip speed ratio can be bounded by the upper and lower limits of the tip speed ratio using nacelle measurements as the Kalman Filter values will lie within the bounds of the measured data. Using the Kalman filtered rotor speed and tip speed ratio, the wind speed can be obtained, as shown in equation (22).

$$U = \frac{R \cdot \omega_r}{\lambda} \#(22)$$

The Kalman filtered wind speed can be bounded by the lower and upper bounds of the nacelle wind speed. Process and measurement noise covariance was tuned at the Kalman filter to reduce noise. The noise covariance of the Kalman filter is tuned to accurately represent the shape of the torque response of the model with that of the data collected from the SWIFT facility. The Kalman filter can over-filter the WSE dynamics, therefore noise can be reintroduced to the system to capture these dynamics. Fig. 6 illustrates a comparison between the measured nacelle wind speed the results obtained from implementing the Kalman filter.

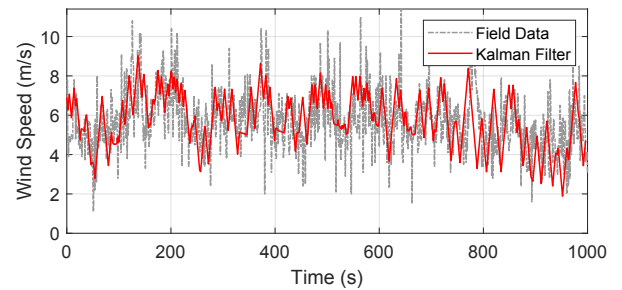


Fig. 6. Comparison between measured nacelle wind speed and Kalman filtered wind speed.

V. MODEL VALIDATION METHODOLOGY

A comparison is made between the proposed WTG model with field measurements from the SWiFT WTGs. The results illustrate that there exists a correlation between the generator torque, generator power and generator speed of the SWiFT facility compared to the WTG model given the nacelle wind speed and the Kalman filtered estimated wind speed. The statistical analysis will consist of the mean absolute error (MAE) as defined in equation (23).

$$MAE = \frac{\sum_{i=1}^n |x - x_i|}{n} \#(23)$$

In this equation, the prediction, true value, and number of samples are denoted as, x, x_i, n . The standard deviation is denoted in equation (24).

$$\sigma = \sqrt{\frac{\sum_{i=1}^n (x_i - MAE)^2}{n}} \#(24)$$

VI. SIMULATION RESULTS

A WTG model that combines both aerodynamics and EMT dynamics is simulated using *MATLAB/Simulink*. Table I summarizes the WTGs control and electrical parameters. Many of the initial values were inherited from models in [3,4]. For this model, the inertia constant is calculated, using equation (5) [11].

$$H = \frac{J \cdot \omega_n}{2 \cdot MVA_{rated}} \#(5)$$

Given the rated values, the calculated inertia time constant is 2.77 s.

TABLE I:
WIND TURBINE GENERATOR PARAMETERS

Parameter	Variable	Value	Units
Rotating inertia	J_r	52,472.5	$kg \cdot m^2$
Gearbox ratio	$GBRatio$	27.5	-
Speed at full load	$\hat{\omega}_g$	1,776.0	RPM
Full load torque	\hat{T}_g	1,603.9	Nm
Synchronous speed	ω_n	1,800	RPM
DC link-bus voltage	V_{DC}	695	V
Nominal power	P_n	200	kVA
Inertia Constant	H	2.77	S
Damping coefficient	K_d	0.01	Pu
Number of pole pairs	P	2	-

Fig. 7 illustrates the comparison between the EMT model and aerodynamic model after tuning the SG, inserting the one-mass model, and including generator torque control. The results demonstrate that the fused model can accurately represent generator dynamics with similar precision to the aerodynamic model that was shown to depict the generator torque better accurately, generator speed and generator power of the WTG. The simulation results comparing the unfiltered wind speed, the post Kalman filtering wind speed and the measured SWiFT WTG field data for generator power, generator speed and

generator torque are illustrated in Fig. 7 through Fig. 10, respectively.

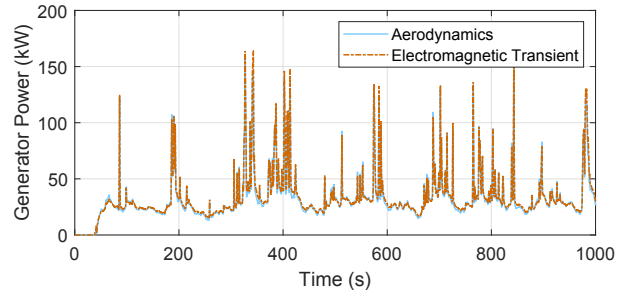


Fig. 7. Results obtained from comparing the generator power of the electromechanical transient model and the aerodynamic model.

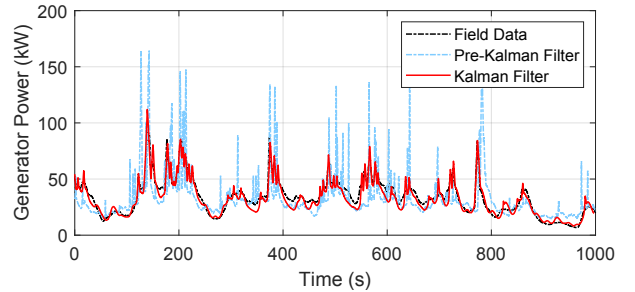


Fig. 8. Results obtained from comparing the generator power of the wind turbine generator model and field data with and without the Kalman filter.

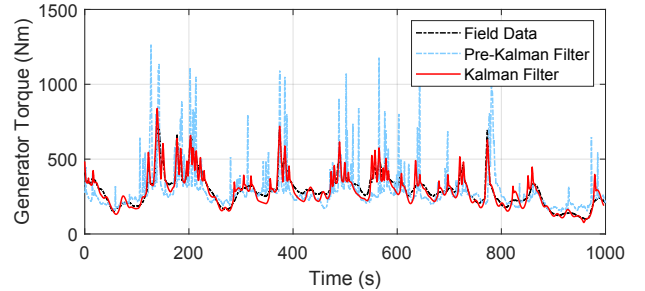


Fig. 9 Results obtained from comparing the generator torque of the wind turbine generator model and field data with and without the Kalman filter.

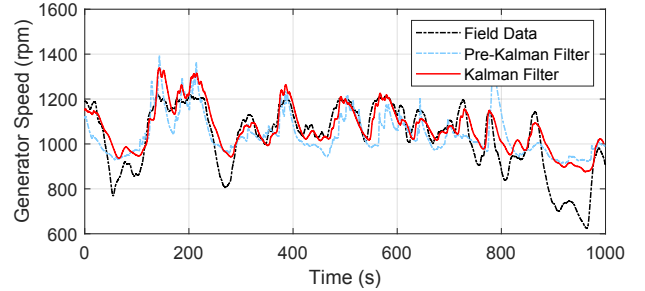


Fig. 10. Results obtained from comparing the generator torque of the wind turbine generator model and field data with and without the Kalman filter.

MAE and STD results are obtained for the 1000 s simulation duration. Table II illustrates the results obtained when comparing the aerodynamic and the EMT models. Table III contains the MAE and standard deviation of results obtained when comparing the model and filed data for generator power, generator speed and generator torque before and after implementing the Kalman filter.

TABLE II:
COMPARISON AERODYNAMIC AND EMT MODELS

Parameter	MAE	STD (σ)
Generator power/speed	5.8	4.5

TABLE III:
COMPARISON BETWEEN MODEL AND SWIFT FIELD DATA

Parameter	MAE		STD (σ)	
	Pre-KF	KF	Pre-KF	KF
Generator power	33.97	15.20	35.57	11.68
Generator speed	9.08	7.71	9.00	8.18
Generator torque	25.64	12.32	29.59	10.20

These results demonstrate that a model using the discussed Kalman filtered wind speed approach can improve model adequacy substantially. The MAE is lower for the generator power, generator speed and generator torque. The lower STD shows that the data is closer to the lower MAE. Therefore, the model is adequate over region II of the WTG power curve.

VII. CONCLUSION

In this paper a *MATLAB/Simulink* power system simulation model that represents the aerodynamics and EMT dynamics of a WTG is presented. The model is designed to represent a SWiFT WTG. The model is validated using measurement data collected from the SWiFT facility. Wind speed from the nacelle contains process and measurement noise, the Kalman filter was used to estimate the true wind speed that exists in front of the rotor. The simulation model demonstrated that by using a single-mass model for aerodynamic torque, torque control from SWiFT to obtain generator torque and estimating the wind speed via Newton-Raphson Kalman filter approach and reconfiguring the SG the system can accurately represent the dynamics measured at the SWiFT facility. Improvements of SG modeling and accurate process/measurement noise can lead to further improvements. More accurate SWiFT data showing a true power curve transition will allow for further model adequacy.

ACKNOWLEDGMENT

Sandia National Laboratories is a multi-mission laboratory managed and operated by National Technology and Engineering Solutions of Sandia, LLC., a wholly owned subsidiary of Honeywell International, Inc., for the U.S. Department of Energy's National Nuclear Security Administration under contract DE-NA-0003525.

This work was sponsored in part by the Consortium for Advanced Synergistic Program for Indigenous Research in Engineering (ASPIRE) from the National Nuclear Security Administration part of the U.S. Department of Energy.

REFERENCES

- [1] T. Ackermann, *et al.*, "Code Shift: Grid Specifications and Dynamic Wind Turbine Models", *IEEE Power and Energy Magazine*, vol. 11, no. 6, pp. 72-82, Oct. 2013.
- [2] A. Ellis, *et al.*, "Generic models for simulation of wind power plants in bulk system planning studies", *IEEE Power and Energy Society General Meeting*, Oct. July 24-28, 2011, pp. 1-8.
- [3] R. Gagnon, *et al.*, "Large-Scale Real-Time Simulation of Wind Power Plants into Hydro-Quebec Power System", *9th International Workshop on Large-Scale Integration of Wind Power into Power Systems as well as on Transmission Networks for Offshore Wind Power Plants*, Jul. 1, 2010, pp. 73-80.
- [4] N. W. Miller, J. J. Sanchez-Gasca, W. W. Price, and R. W. Delmerico, "Dynamic Modeling of GE 1.5 and 3.6 MW Wind Turbine-Generators for Stability Simulations", *IEEE Power Engineering Society General Meeting*, 2003, pp. 1977-1983.
- [5] M. Asmine, *et al.*, "Model Validation for Wind Turbine Generator Models", *IEEE Transaction on Power Systems*, vol. 26, no. 3, pp. 1769-1782, Aug. 2011.
- [6] M. Singh, and S. Santoso, "Dynamic Models for Wind Turbines and Wind Power Plants", *National Renewable Energy Laboratory Technical Report*, pp.1-115, Jan. 2011.
- [7] A. Ellis, Y. Kazachkov, E. Muljadi, P. Pourbeik and J. J. Sanchez-Gasca, "Description and Technical Specifications for Generic WTG Models — A Status Report," *IEEE/PES Power Systems Conference and Exposition*, Mar. 20-23, 2011, pp. 1-8.
- [8] J. Jonkman, and K. Shaler, "FAST User's Guide and Theory Manual", *National Renewable Energy Laboratory (NREL) Technical Report*, pp.1-70, Apr. 2021.
- [9] N.S. Cetin, *et al.*, "Assessment of Optimum Tip Speed Ratio of Wind Turbines", *Mathematical and Computational Applications*, vol. 10, no. 1, pp. 147-154, Apr. 1, 2005.
- [10] A.K. Singh, and R. Krisham, Y. Sood, "Modeling and Control of Grid Connected Variable Speed PMSG Based Wind Energy System", *Conference on Advances in Communication and Control Systems*, Apr. 6-8, 2013, pp. 134-139.
- [11] F. Sun, *et al.*, "Measurement Method of Inertia Constant of Power System Based on Large-Scale Wind Power Grid Connection", *Energy Reports*, vol. 8, no. 6, pp. 200-209, Mar. 2022.
- [12] P. Pourbeik, *et al.*, "Generic Stability Models for Type 3 & 4 Wind Turbine Generators for WECC", *IEEE Power & Energy Society General Meeting*, July 21-25, 2013, pp. 1-5.
- [13] R. T. Smith, "Synchronous and Induction Machines", *Analysis of Electrical Machines*, 1st Edition (revised), Netherlands, Elsevier Science & Technology, Oct. 2013, ch. 3, pp. 100-109.
- [14] D. Song, J. Yang, M. Dong, and Y.H. Joo, "Kalman Filter-based Wind Speed Estimation for Wind Turbine Control", *International Journal of Control, Automation and Systems*, vol. 15, no. 3, pp. 1089-1096, Jun. 2017.
- [15] D. Jena, and S. Rajendran, "A Review of Estimation of Effective Wind Speed-Based Control of Wind Turbines", *Renewable and Sustainable Energy Reviews*, vol. 43, pp. 1046-1062, Mar. 2015.
- [16] Y. Nam, *et al.*, "Feedforward Pitch Control Using Wind Speed Estimation", *Journal of Power Electronics*, vol. 11, no. 2, pp. 211-217, Mar. 2011.
- [17] P. Matisko, and V. Havlena, "Noise Covariances Estimation for Kalman Filter Tuning", *Adaptation and Learning in Control and Signal Processing*, Aug. 26-28, 2010, pp. 1-6.
- [18] S. W. Chang, G. C. Goodwin, and K. S. Sin, "Convergence Properties of the Riccati Difference Equation in Optimal Filtering of Nonstabilizable Systems", *IEEE Transaction on Automatic Control*, vol. 29, no. 2, pp. 110-118, Feb. 1984.
- [19] J. G. Gonzalez-Hernandez, and R. Salas-Cabrerera, "Representation and estimation of the power coefficient in wind energy conversion systems", *Revista Facultad de Ingeniería*, vol. 28, no. 50, pp. 77-90, Jan. 2019.